Ab Initio Molecular Dynamics Study of Adsorption Sites on the (001) Surfaces of 1:1 Dioctahedral Clay Minerals

Daniel Tunega,*,†,‡ Lubomir Benco,§ Georg Haberhauer,† Martin H. Gerzabek,† and Hans Lischka‡

Austrian Research Centers Seibersdorf, A-2444 Seibersdorf, Austria, Institute for Theoretical Chemistry and Structural Biology, University of Vienna, Währingerstrasse 17, A-1090 Vienna, Austria, and Institute for Material Physics and for Computational Materials Science, University of Vienna, Sensengasse 8, A-1090 Vienna, Austria

Received: June 27, 2002; In Final Form: September 9, 2002

Ab initio molecular dynamics room-temperature simulations and full relaxation of atomic positions are performed in the study of adsorption sites on the octahedral and tetrahedral surfaces (parallel to the (001) plane) of the kaolinite group of clay minerals. Interactions of water and acetic acid molecules with both surfaces are investigated. Simulations showed that both polar molecules are strongly bound to the octahedral surface forming several simultaneous hydrogen bonds. Surface hydroxyl groups located at the octahedral surface act as proton donors as well as proton acceptors demonstrating their amphoteric character. Moreover, proton jumps between the carboxyl group of acetic acid and one surface hydroxyl group were observed in the molecular dynamics simulations. On the other hand, both molecules interact only very weakly with the tetrahedral side of the kaolinite layer showing the hydrophobicity of this surface. The octahedral surface is hydrophilic.

Introduction

Clay minerals form a major part of the inorganic matter of soils and affect significantly the physicochemical processes occurring there. They exist in the form of very small particles (∼2 μm in diameter) with different morphology and have a high specific surface area and a high chemical surface activity with respect to interactions with various solutions. Since interactions of clay minerals with aqueous solutions are of great relevance for industrial and/or natural processes, a detailed understanding of these processes is very important. These interactions occur as sorption of solute and/or solvent molecules on to mineral surfaces and additionally as an intercalation into the interlayer space.

Organic acids frequently occur in soils since these acids arise as final products of several, complicated biochemical degradation processes. They either form various associates or complexes in soil solutions or can be adsorbed on inorganic or organic solid particles. Organic acids also participate in the dissolution processes of soil minerals.[1−4] Therefore, numerous experimental investigations have been undertaken in order to obtain understanding of clay mineral−solution interactions.[5] However, it is difficult to obtain from experimental investigations detailed information of molecular structures and dynamical behavior at such clay-solution interfaces. Quantum-chemical modeling calculations can give, e.g., interesting insight concerning a structural characterization of adsorption sites and of interactions between surfaces and adsorbed molecules.

The present work is a continuation of our recent investigation of adsorption sites on (001) surfaces of kaolin group minerals,[6] where we had used a cluster model approach and density functional theory (DFT) as computational method. In that previous work, the structural and energy characteristics of the adsorption of molecules, such as water, acetic acid, and acetate anion, on the (001) tetrahedral and octahedral surfaces of a kaolinite layer were investigated. The interaction sites were characterized and structures and bonding of the adsorption complexes were described. It was found that the water molecule and the acetate anion form several strong hydrogen bonds with surface hydroxyl groups on the octahedral side while in the case of the tetrahedral side only very weak hydrogen bonds were observed. Corresponding interaction energies differ significantly for both surfaces also.

The advantage of the finite cluster approach used in our previous study[6] was the availability of a large multitude of quantum chemical methods (ab initio and DFT) and standard molecular program packages allowing highly accurate computations of interaction energies and cluster structures. The finite cluster approach has been used many times in aluminoslilicate chemistry as it is documented in several reviews.[7−9] To avoid artificial edge effects the geometry of the outer part of the clay cluster was held fixed at the structure of the kaolinite mineral and only the geometry of the innermost part representing the adsorption site was optimized. The main disadvantages of the cluster approach are the limited cluster size, missing long-range interactions between the cluster and the rest of the solid bulk, which had been left out, and the just-mentioned necessity to keep some part of the cluster rigid. This latter restriction prohibits the determination of global energy minima and the consistent calculation of spectroscopic and thermodynamic properties.

In this work we have used methods employing translational symmetry in order to avoid the just-mentioned deficiencies.

* To whom correspondence should be addressed. E-mail: Daniel.Tunega@univie.ac.at. FAX: +43-1-4277-9527. Permanent address of Daniel Tunega and Lubomir Benco: Institute of Inorganic Chemistry, Slovak Academy of Sciences, Dúbravská cesta 9, SK-84236 Bratislava, Slovakia.

† Austrian Research Centers Seibersdorf.

‡ Institute for Theoretical Chemistry and Structural Biology.

§ Institute for Material Physics and for Computational Materials Science.

10.1021/jp026391g CCC: $22.00
Published on Web 10/10/2002

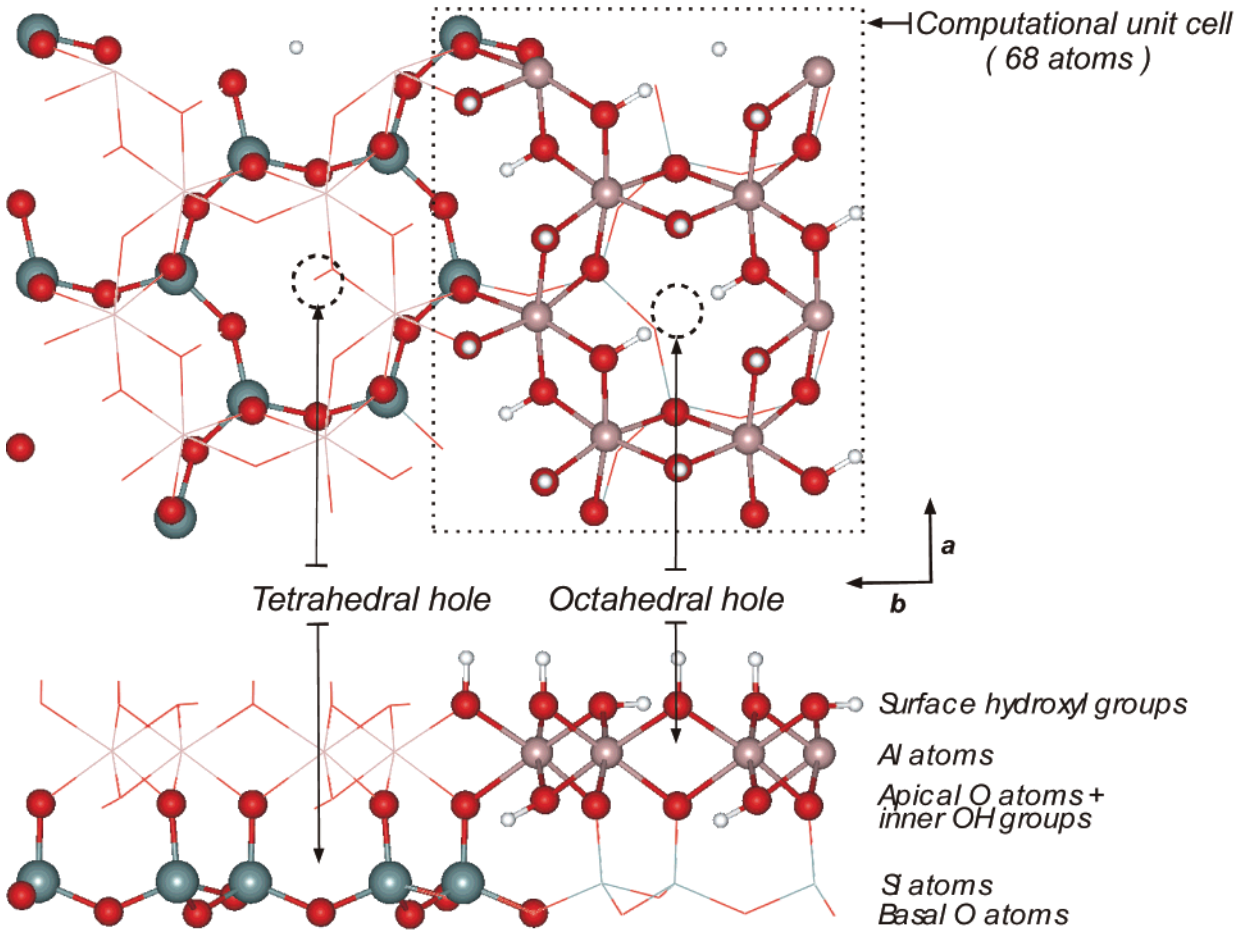

Figure 1. Structure of the kaolinite layer. Top (upper) and side (lower) views. Computational unit cell and interaction sites are also depicted.

These methods describe periodic structures properly without any structural simplification and permit full structural relaxations including unit cell parameters. However, for the description of local defects perturbing the translational symmetry usually larger computational unit cells (twice or more) have to be used as compared to the original structural unit cell of the unperturbed crystal. The purpose of our present investigations is to use ab initio molecular dynamics techniques[10−14] to describe the dynamical behavior of the adsorbed molecules and to perform comparisons between the two chemically different surfaces of the kaolinite layer demonstrating the importance of surface hydroxyl groups in the sorption processes.

Structural and Computational Details

Typical representatives of the kaolinite group minerals are kaolinite and dickite. These minerals possess a 1:1 dioctahedral structure[15] and have a common chemical formula $Al_2Si_2O_5(OH)_4$. The only difference between kaolinite and dickite is in the layer stacking. Individual layers are identical and consist of two connected sheets (see Figure 1): a tetrahedral one formed from SiO_4 tetrahedra and an octahedral one formed from AlO_6 octahedra sharing edges. Both sheets are connected via a plane of apical oxygen atoms. The SiO_4 tetrahedra are connected such that they form ditrigonal tetrahedral holes (Figure 1) in the tetrahedral sheet and the surface of this sheet is formed from basal oxygen atoms. One-third of all possible octahedral central positions in the octahedral sheet are empty. Therefore, cavities are formed also in the octahedral sheet (octahedral holes in Figure 1). The surface of the octahedral sheet is covered with surface hydroxyl groups, which are involved in hydrogen bonds with basal oxygen atoms of the adjacent layer. Thus, the kaolinite layer has two different surfaces: a tetrahedral one formed from the basal oxygen atoms and an octahedral one formed from surface hydroxyl groups. Both these surfaces are parallel to the crystallographic (001) surface and form the major part of the surface of crystal particles what was confirmed by scanning electron microscopy and atomic force microscopy studies.[16] The interlayer space in kaolinite and dickite is empty and the total charge of layers is zero. Figure 1 presents two different views (top and side) of the structure of the single kaolinite layer. Different atomic planes and existing octahedral and tetrahedral holes are also depicted in Figure 1. As was found in our previous investigation,[6] the aforementioned holes in the tetrahedral and octahedral surfaces are favorable interactions sites for adsorption of small polar molecules.

For the study of adsorption sites on the (001) surfaces, a single kaolinite layer derived from the structure of the mineral dickite was chosen. Dickite has a monoclinic structure with lattice parameters $a = 5.138$ Å, $b = 8.818$ Å, $c = 14.389$ Å, and $\beta = 96.7°$[17] and has two layers in the unit cell. Since we wanted to study surface properties of a single layer only we removed one layer from the dickite structure and increased the c lattice parameter to 21 and 26.4 Å, respectively, to minimize interactions between adsorbed molecules and upper layer. Since the thickness of the single layer is about 5.4 Å, an empty space of about 15.6 and 21 Å, respectively, above the layer surfaces was created. The difference in the adsorption energy obtained from static structural relaxations was less than 1.5% between these two choices of the empty interlayer space. According to this result we decided to perform all molecular dynamics calculations

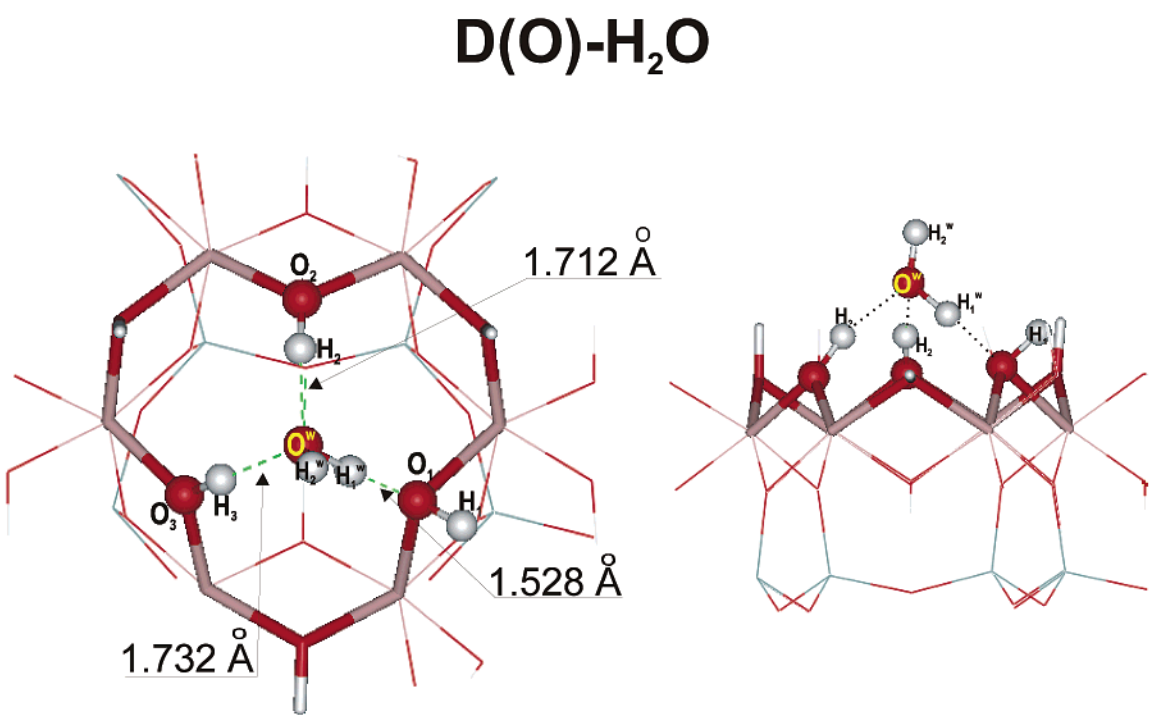

Figure 2. Two views on the H_2O molecule interacting with the octahedral side of the kaolinite layer. The lengths of hydrogen bonds obtained from static relaxations are given in the figure.

using the smaller interlayer spacing of 15.6 Å since calculations with the bigger computational unit cell are considerably more demanding. Additionally, we doubled the lattice parameter *a* since we wanted to study the adsorption of individual molecules on the clay surfaces and minimize the interactions between equivalent molecules in neighboring cells. Using this computational unit cell, six empty sites of the same kind surround an adsorption site above tetrahedral or octahedral holes. The computational unit cell projected onto the $a \times b$ plane is depicted in Figure 1 and contains 68 atoms (excluding the absorbed molecule). Since we studied the adsorption of the water and acetic acid molecules on both surfaces (octahedral and tetrahedral) we investigated in total four cases: octahedral side-water (denominated D(O)-H_2O), tetrahedral side-water (D(T)-H_2O), octahedral side-acetic acid (D(O)-HAc), and tetrahedral side-acetic acid (D(T)-HAc). As initial positions for the static relaxations and the molecular dynamics simulations the structures obtained in the previous cluster calculations[6] were taken.

Ab initio periodic total-energy geometry optimizations and molecular dynamics simulations were performed to obtain both fully relaxed structures and dynamical properties. The calculations have been performed using the Vienna ab initio simulation package (VASP).[18,19] VASP performs an iterative solution of the Kohn−Sham equations of density functional theory[20] on the basis of the minimization of the norm of the residual vector to each eigenstate and an efficient charge density mixing. For the exchange-correlation functional, both the localized density approximation (LDA) and the generalized gradient approximation (GGA) have been used. The LDA is parametrized according to Perdew−Zunger[21] and the GGA according to Perdew−Wang.[22] The calculations are performed in a plane-wave basis set using the projector-augmented wave (PAW) method[11,23] and ultrasoft pseudo-potentials.[24,25] The PAW method combines the advantage of the plane-wave basis set with the accuracy of the all-electron schemes. For the static structural relaxation in fixed unit cell parameters, we used a plane-wave cutoff energy of 350 eV representing a high-precision quality of the calculation. Since the computational unit cell is sufficiently large, the Brillouin-zone sampling is restricted to the Γ point, using modest smearing of the eigenvalues to improve total energy convergence. The optimization of atomic positions is performed using a conjugate-gradient algorithm with a stopping criterion of 10^{-5} eV for the total energy. No symmetry restrictions were applied during the relaxation procedure. Adsorption energies were calculated as the difference between the total electronic energies of the whole system and the corresponding subsystems (layer, adsorbed molecule). Both subsystems were fully optimized also under the same conditions as those for the whole system. This means that the isolated layer and the adsorbed molecules were allowed to relax in the same fixed computational unit cell.

Fixed-volume molecular dynamics simulations were performed. The finite-temperature simulation of the dynamical properties was done at 300 K. In the dynamics calculations a canonical ensemble with a Nosé thermostat procedure[26] was used. The Verlet velocity algorithm[27] with a time step Δt of 1 fs was chosen, and a simulation time of 2 ps was used. The densities of phonon states were calculated using Fourier transformation of the velocity autocorrelation function. Molecular dynamics simulations were performed using the plane-wave cutoff energy of 200 eV representing a somewhat lower precision than that used in the static relaxations. The accuracy of both cutoffs is discussed below using D(O)-H_2O as the test case.

Results and Discussion

Static Relaxations. *D(O)-H_2O.* Figure 2 shows an adsorbed water molecule on the octahedral surface. Three surface hydroxyl groups surrounding the octahedral hole are involved in the formation of the hydrogen bonds. Two of them act as proton donors to the water oxygen atom, the third one as proton acceptor. The latter bond is relatively strong as indicated by its length of 1.53 Å (see Table 1, static relaxation, energy cutoff of 350 eV). The other two hydrogen bonds with lengths of about 1.72 Å are significantly longer. Similar results were obtained also in our cluster model calculations[6] (see Table 1). For

TABLE 1: Comparison of Calculated Structural Parameters for the D(O)-H_2O System Obtained from the Cluster Calculations[6] (ONIOM(B3LYP/SVP:PM3 Method) and the Present Study Using Two Values for the Energy Cutoff Parameter

structural parameter[a]	cluster model	static relaxation		molecular dynamics	
		200 eV	350 eV	200 eV	350 eV
$H_1^w-O^w$	0.997	1.034	1.048	1.027	1.039
$H_2^w-O^w$	0.965	0.980	0.987	0.982	0.989
$H_1^w-O^w-H_2^w$	105.8	111.1	110.4	110.3	109.8
$H_1^w\cdots O_1$	1.628	1.541	1.528	1.621	1.590
$O^w\cdots H_2$	1.886	1.730	1.712	1.802	1.817
$O^w\cdots H_3$	1.957	1.737	1.732	1.826	1.816
O_1-H_1	0.987	0.988	0.995	0.988	0.997
O_2-H_2	0.973	0.993	0.997	0.991	0.998
O_3-H_3	0.970	0.992	0.998	0.992	1.000
$O^w\cdots O_1$	2.615	2.571	2.572	2.632	2.610
$O^w\cdots O_2$	2.917	2.713	2.699	2.763	2.778
$O^w\cdots O_3$	2.815	2.710	2.709	2.778	2.775
$O_1\cdots H_1^w-O^w$	169.7	173.7	173.5	168.4	167.4
$O_2-H_2\cdots O^w$	171.2	170.1	169.6	164.4	163.8
$O_3-H_3\cdots O^w$	159.7	166.0	165.3	161.9	162.2

[a] Bond lengths and interatomic distances are in angstroms; angles are in degrees. Labeling of atoms corresponds to labeling in Figures 2−5.

comparison, in the last two columns of Table 1 mean values of structural parameters obtained in the molecular dynamics simulations with two different energy cutoff parameters are given as well. The changes in the geometrical parameters obtained in the static relaxation calculations using two different energy cutoff parameters are about 1.5%, which is an acceptable difference. A similar discrepancy is also observed for the mean values obtained in the MD simulations. More details about structural changes of the adsorbed water molecule will be discussed later in this work. The calculated adsorption energies are more sensitive to the energy cutoff: the adsorption energy is −13.1 kcal/mol for an energy cutoff of 200 eV, while it is −14.7 kcal/mol for a 350 eV energy cutoff. The difference between both values is about 8%. These results show that a higher accuracy in terms of cutoff energy is required for the calculation of interaction energies than for geometries. Both values for the interaction energy are larger in absolute value than the one obtained with the cluster model calculation[6] (−10.5 kcal/mol at the ONIOM(B3LYP/SVP:PM3) level of the theory). This discrepancy is acceptable since in the cluster model calculations long range Coulombic interactions between polar molecule and the "missing" part of the solid surface of the mineral are not taken into account. Moreover, this comparison is only approximate since results of two different approaches (B3LYP method in the cluster calculation and LDA-GGA approach in the plane-wave basis set) are compared.

D(T)-H_2O. Figure 3 presents the optimized structure of water adsorbed to the plane of the basal oxygen atoms of the tetrahedral side. In this case water is located approximately above the middle of the ditrigonal hole and both water protons direct to the surface. Only very weak hydrogen bonds are formed between the basal oxygen atoms and water protons. The lengths of these bonds are given in Figure 3 and are larger than 2.6 Å. These results differ more from the cluster model calculations[6] than those in the previous case D(O)-H_2O. In the cluster model simulation, the water molecule was shifted toward two basal oxygen atoms and two shorter hydrogen bonds (about 2.3 Å) were formed than in the present case. In the adsorption of the water molecule on the tetrahedral side, the structure of the water molecule changes only little. The adsorption energy of −4.1 kcal/mol is much smaller in absolute value than that for the water adsorbed to the octahedral surface. From the cluster model study we obtained −3.8 kcal/mol at the ONIOM(B3LYP/SVP:PM3) level.

D(O)-HAc. Adsorption of the acetic acid molecule was not investigated in our previous investigation.[6] The choice of the initial geometry was derived from the adsorption of the acetate anion on the octahedral surface.[6] The adsorbed acetic acid molecule is located above the surface in such a way that the C−C bond is almost perpendicular to the (001) plane and the CH_3 group is directed away from this plane (see Figure 4). Four hydrogen bonds are formed between the carboxyl group and the surface hydroxyl groups. The carbonyl oxygen (O_2^a) acts as the proton acceptor and forms three hydrogen bridges: two shorter ones (about 1.8 Å) and one longer one (about 1.9 Å). On the other hand, the OH group of the carboxyl group acts as proton donor and forms a strong hydrogen bond with a short contact (1.45 Å) with one oxygen atom of the surface hydroxyl group (O_4 in Figure 4). Sterical and structural arrangements of the hydroxyl groups surrounding the octahedral hole and of the acetic acid molecule allow a relatively strong binding of the HAc molecule to the octahedral surface. The calculated adsorption energy of −20.8 kcal/mol reflects the number and the nature of the formed hydrogen bonds. Thus, the HAc molecule is adsorbed stronger to the octahedral surface than the water molecule. The structure of the adsorbed acetic acid molecule is modified significantly with respect to the isolated molecule as will be described in detail in the "Molecular dynamics Simulations" subsection.

D(T)-HAc. The situation of the adsorption of the acetic acid molecule on the tetrahedral surface (Figure 5) is very similar to that of the water molecule at this surface. Again, the HAc molecule is localized above the ditrigonal tetrahedral hole with the C−C bond almost perpendicular to the tetrahedral plane and with the CH_3 group directed out from this plane. Only the proton of the carboxyl group interacts weakly with one of the basal surface atoms (O_1 in Figure 5) and a single, relatively weak hydrogen bond with a length of 2.02 Å is formed. The same position of the acetic acid molecule was found also in our cluster model study[6] with a bond length of 1.94 Å for the hydrogen bond. The carbonyl oxygen atom (O_2^a) of the acetic acid molecule is located in a distance of more than 3.5 Å from the nearest basal oxygen atoms indicating predominant repulsive interactions. The calculated interaction energy of −2.0 kcal/mol reflects the weak interaction between the HAc molecule and the tetrahedral plane. This value is similar to the one of −2.6 kcal/mol obtained in the cluster model calculation[6] at the ONIOM(B3LYP/SVP:PM3) level of the theory.

Molecular Dynamics Simulations. In this subsection, the dynamical behavior of the adsorbed molecules is described. For the purpose of comparison, molecular dynamics simulations of the isolated, free H_2O and HAc molecules under the same conditions (same computational unit cell, energy cutoff, etc.), as for the entire system (surface plus adsorbed molecule) were performed as well. Molecular dynamics simulation of the free isolated kaolinite layer has been investigated previously[28,29] and is not discussed in this paper.

Average values and the shape of the time evolution curves for the OH stretching and the HOH bending modes of the water molecule in the D(T)-H_2O system are practically unchanged comparing to free water molecule. On the other hand, the vibrational characteristics are changed significantly for the water adsorbed to the octahedral surface (Figure 6). The $O^w-H_1^w$ bond of the water molecule involved in the hydrogen bond with the surface hydroxyl group O_1H_1 (see Figure 2) is stretched

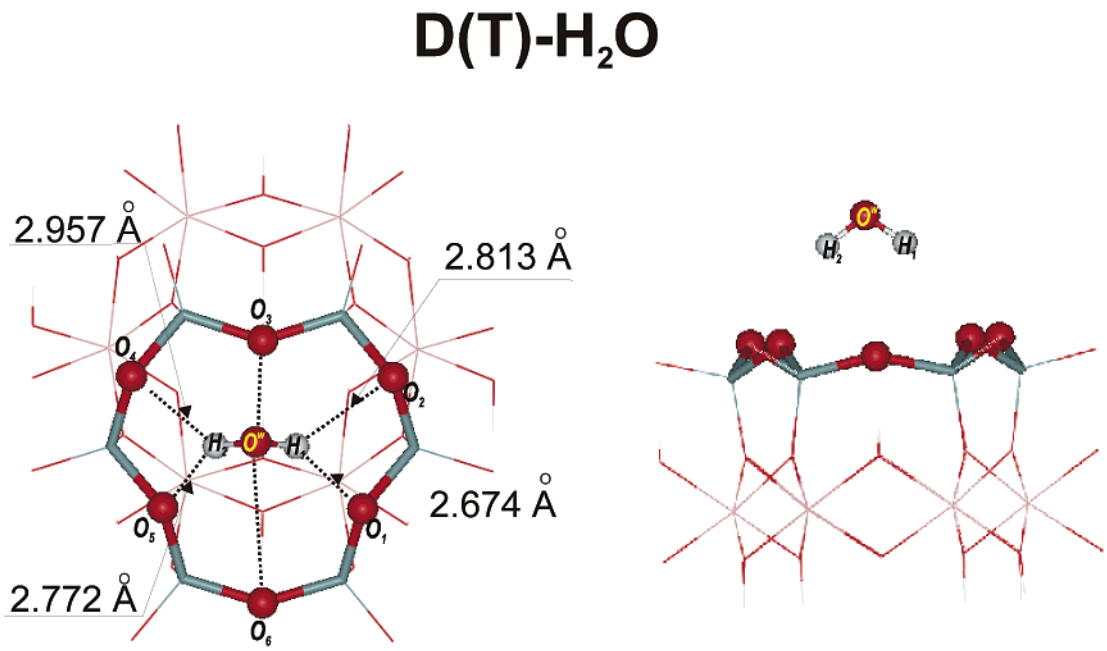

Figure 3. Two views on the H_2O molecule interacting with the tetrahedral side of the kaolinite layer. The lengths of hydrogen bonds obtained from static relaxations are given in the figure.

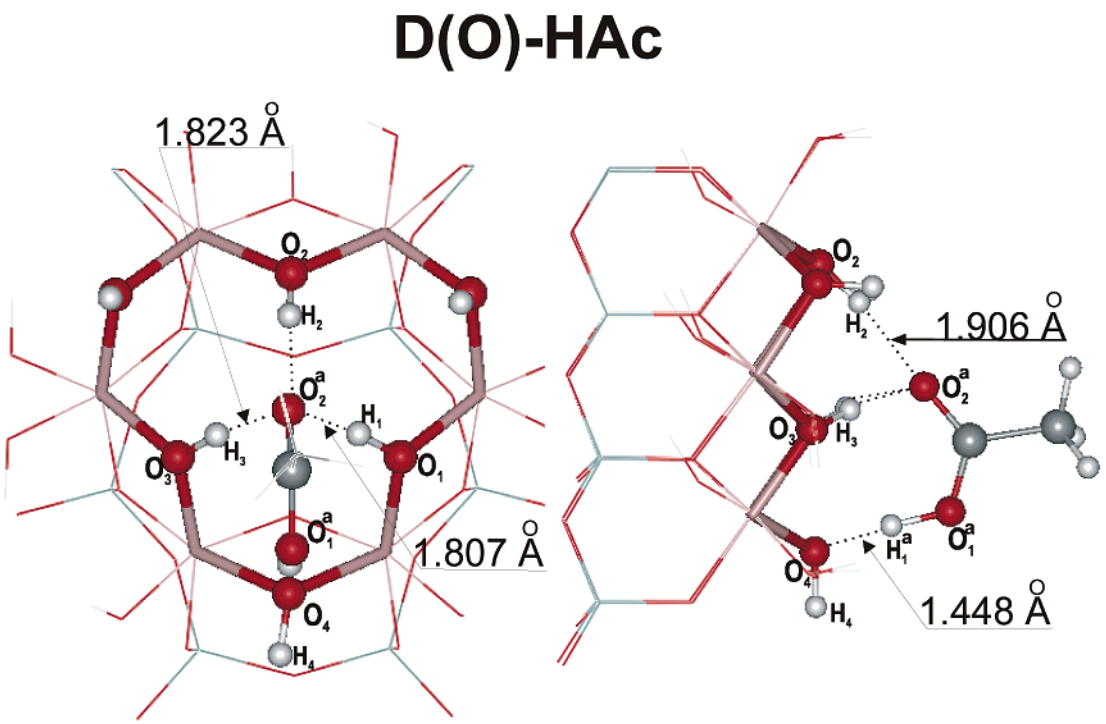

Figure 4. Two views on the HAc molecule interacting with the octahedral side of the kaolinite layer. The lengths of hydrogen bonds obtained from static relaxations are given in the figure.

significantly (with a mean value of 1.027 Å) and the amplitudes of the oscillations are larger than in the case of the free water molecule. The O−H bond of the water molecule not involved in any hydrogen bond ($O^wH_2^w$ in Figure 2) is slightly shorter (with the mean value of 0.982 Å) in comparison to the free water molecule (the mean value of 0.985 Å) and its amplitudes of the oscillations are smaller. For D(O)-H_2O, the mean value of the water bond angle of 110.3° differs significantly from that for the free water molecule (105.6°). Figure 7 displays the dynamics of the three surface hydroxyl groups involved in hydrogen bonds and corresponding O···H distances in the D(O)-H_2O system. The dynamical characteristics reflect the already described fact that two of those surface hydroxyl groups act as proton donors (O_2H_2 and O_3H_3) while the third one, O_1H_1, acts as proton acceptor. The average bond lengths of O_2H_2 and O_3H_3 groups compared to the O_1H_1 group are slightly larger. Comparison to the free kaolinite layer[28] showed that variations in the bond lengths of OH groups involved in hydrogen bonds are very small (calculated values for free surface hydroxyl groups are in the interval 0.985−0.993 Å).

A comparison of the vibrational behavior of the $O^wH_2^w$ (see Figure 6) and O_1H_1 (see Figure 7) groups shows not unexpected similarities. Amplitudes of oscillations of both OH groups are much smaller in comparison to amplitudes of the other OH

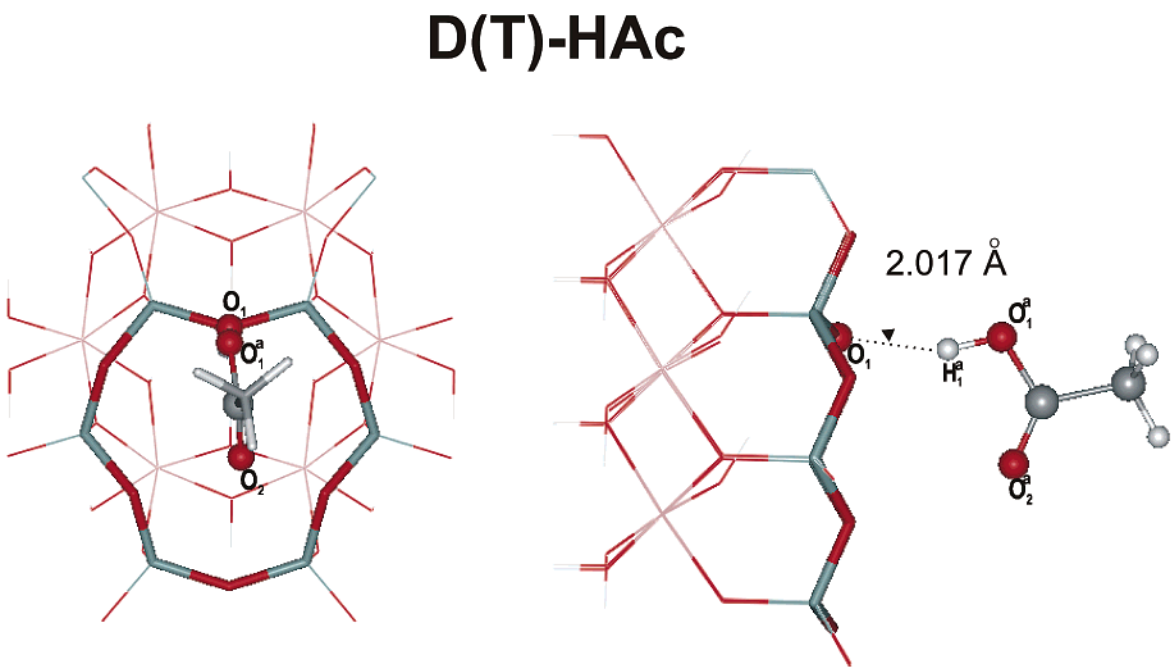

Figure 5. Two views on the HAc molecule interacting with the tetrahedral side of the kaolinite layer. The lengths of hydrogen bonds obtained from static relaxations are given in the figure.

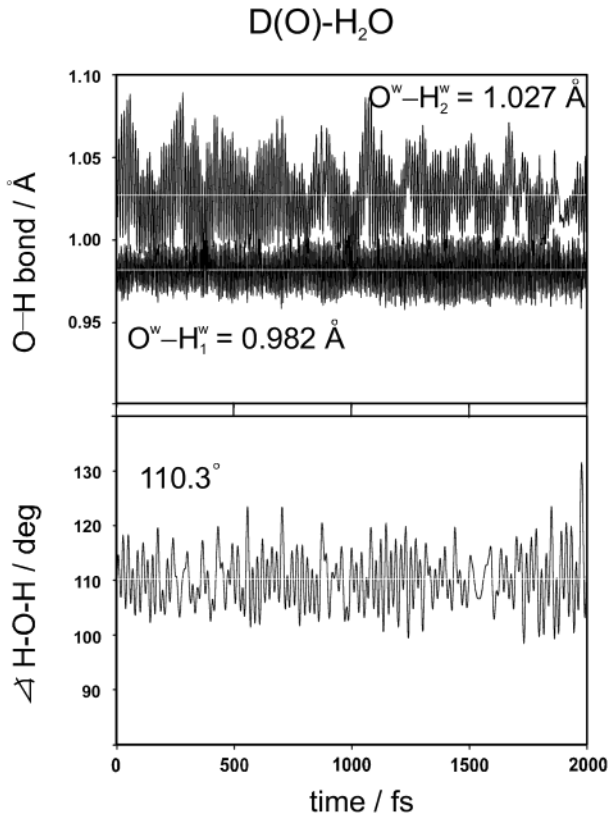

Figure 6. Time evolution curves for the OH stretching and the HOH bending vibrations of the water molecule interacting with the octahedral surface. Horizontal lines indicate mean values and correspond to the numbers given in the figure.

groups. This is the consequence of the fact that both protons (H_1 and $H_2{}^w$) do not participate in hydrogen bonds. In case of the three O···H bonds (curves d), e) and f) in Figure 7), the two hydrogen bonds between the water oxygen atom and the two hydrogen atoms H_2 and H_3 are very similar, having mean values of about 1.8 Å. The third hydrogen bond between the water proton $H_1{}^w$ and the O_1 atom of the surface OH group is again different. Its mean value is about 1.62 Å. However, the oscillatory behavior is similar for all three hydrogen bonds.

Figure 8 depicts the time evolution of the interatomic distances between the surface basal oxygen atoms and the water protons involved in the weak hydrogen bonds between the tetrahedral surface and the water molecule (for labeling see Figure 3). Large and slow oscillations are observed where the very weak hydrogen bonds are spontaneously broken and created by translational−rotational movement of the water molecule above the ditrigonal−tetrahedral hole. At the simulation temperature of 300 K the kinetic energy is higher than rotational barriers of the water molecule in the flat potential energy surface above the tetrahedral hole. Figure 9 also supports this conclusion, where the time evolution of the distances between the water oxygen atom and two basal surface atoms (O_3 and O_6) is depicted (two upper curves). The bottom curve is given for comparison and represents the time evolution of the $O_1\cdots O_w$ distance in the D(O)-H_2O system. Clear differences between the D(O)-H_2O and D(T)-H_2O systems are observed. While the curve for the D(O)-H_2O system indicates a water molecule strongly bound to the octahedral surface because of small amplitude changes, the two upper curves for the D(T)-H_2O case point to a weakly interacting water molecule with large amplitude changes.

The interaction of acetic acid with the tetragonal side (D(T)-HAc) shows a similar scenario as was found for the just-discussed case of D(T)-H_2O. The structural parameters for the HAc molecule in the D(T)-HAc system are changed only very little in comparison to the free HAc molecule. The mean values for the OH, C═O and C−O(H) bonds are about 0.99, 1.22 and 1.40 Å in both cases and also corresponding vibrational patterns are very similar. On the other hand, corresponding structural parameters are strongly perturbed in the D(O)-HAc system. In Figure 10, the time evolutions of the bonds in the carboxyl group are displayed. Curve a) in Figure 10 shows the vibrations of the proton of the carboxyl group. Some very large amplitudes are observed, which indicate the deprotonization of the carboxyl group. More details will be discussed later. The C═O bond involved in the formation of the three hydrogen bonds is

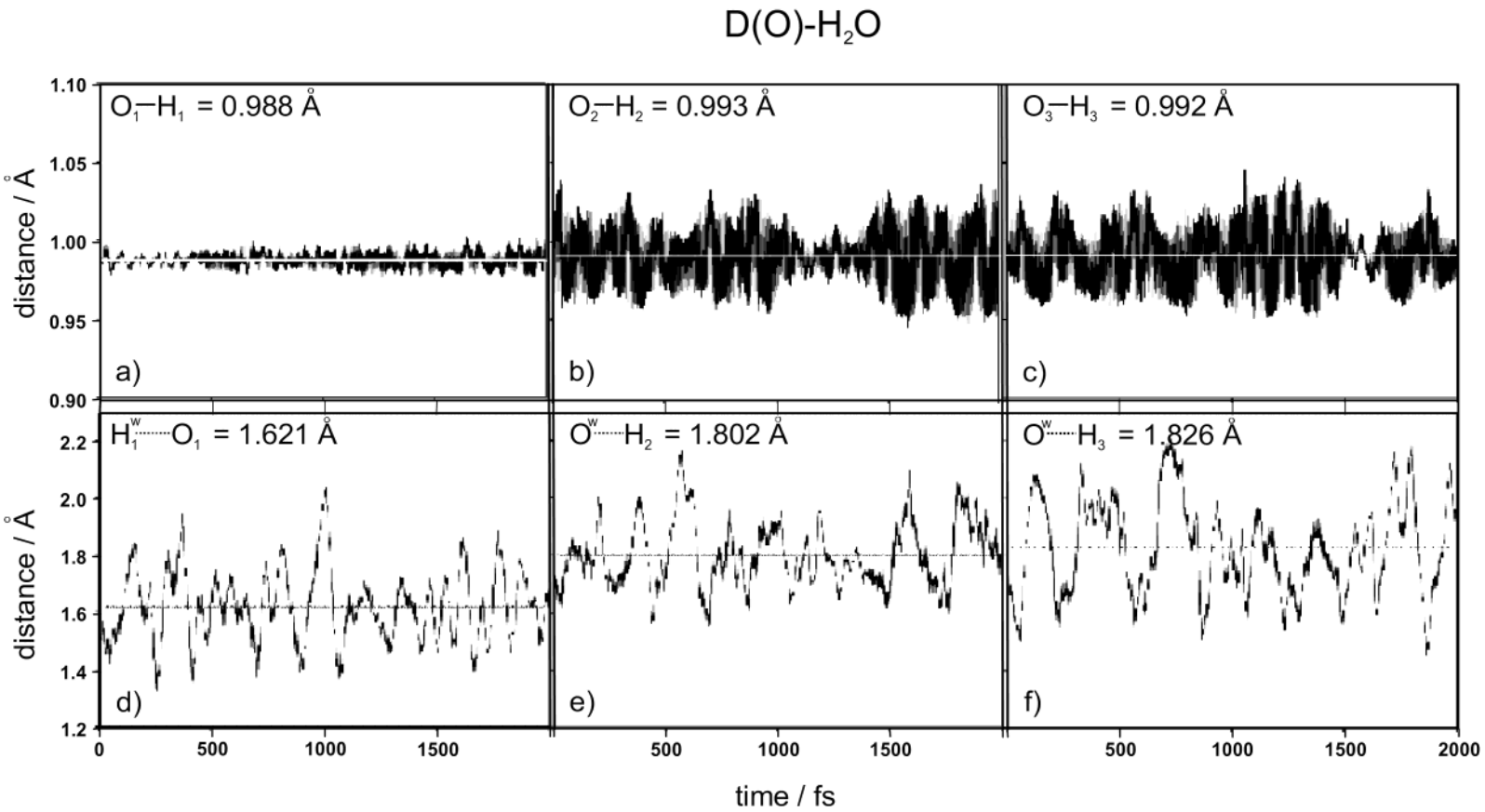

Figure 7. The dynamics of three surface hydroxyl groups involved in hydrogen bonds and corresponding O···H distances in the D(O)-H_2O system. Horizontal lines indicate mean values and correspond to the numbers given in the figure.

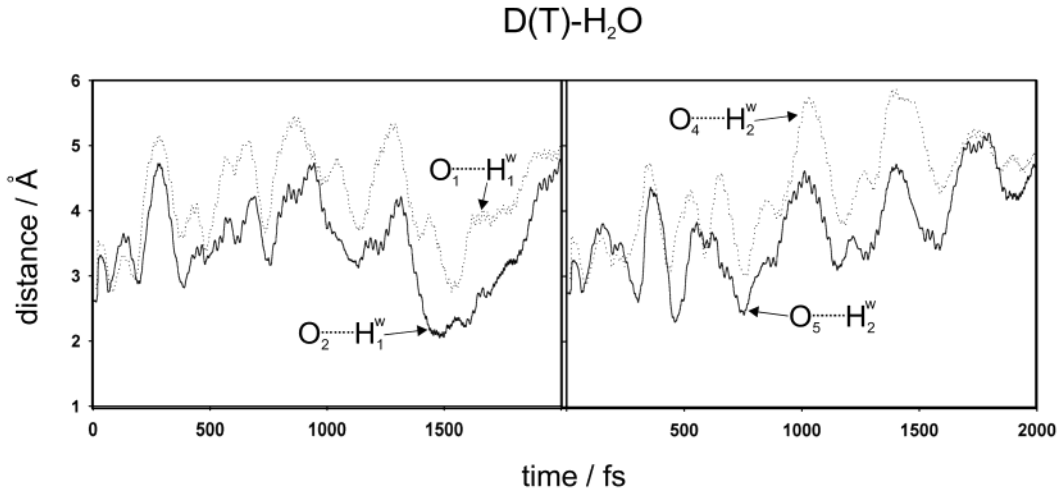

Figure 8. The time evolution of the interatomic distances between the surface basal oxygen atoms and the water protons involved in the weak hydrogen bonds between the tetrahedral surface and the water molecule (labeling according Figure 3).

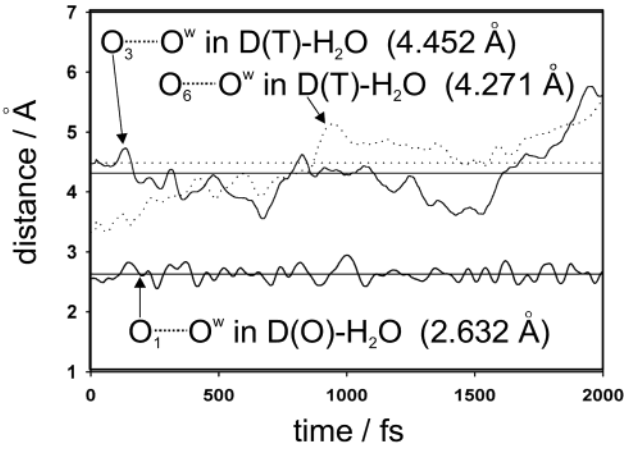

Figure 9. The time evolution of the distances between the water oxygen atom and two basal surface atoms (O_3 and O_6) in the D(T)-H_2O system (two upper curves). The bottom curve represents the time evolution of the $O_1\cdots O_w$ distance in the D(O)-H_2O system. Horizontal lines indicate mean values and correspond to the numbers given in the figure.

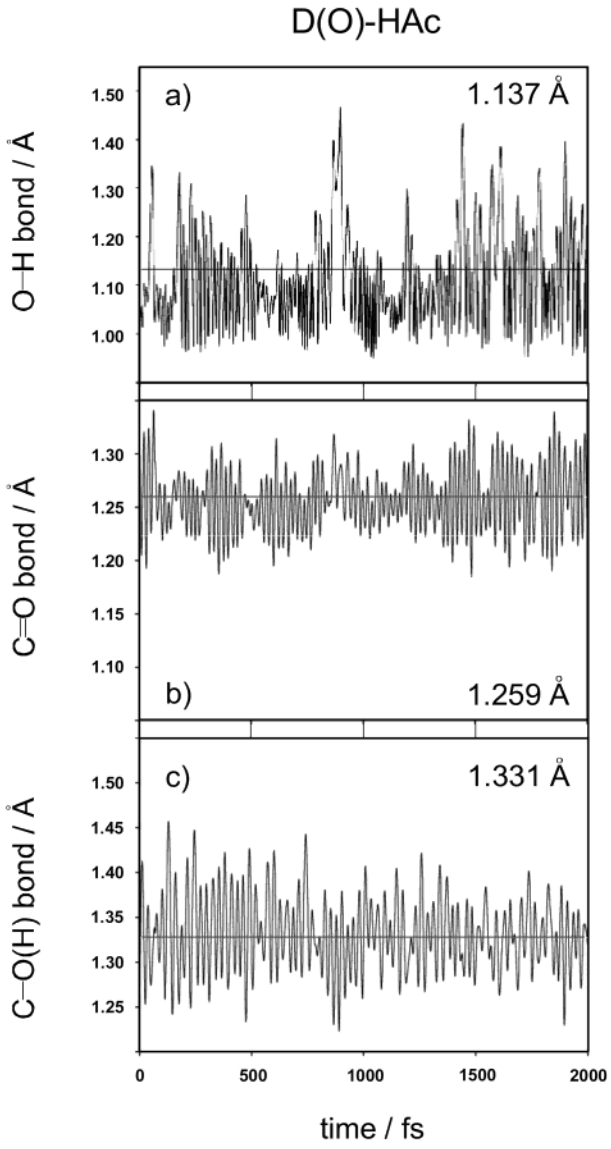

Figure 10. The time evolution of the bonds in the carboxyl group of the D(O)-HAc system. Horizontal lines indicate mean values and correspond to the numbers given in the figure.

stretched by ≈0.04 Å in comparison to the free HAc molecule. On the other hand, C−O(H) bond is significantly shortened in comparison to the free HAc molecule due to strong weakening of the O−H bond of the carboxyl group.

Figure 11 displays the time evolution of the three hydrogen bonds formed between three surface hydroxyl groups and the carbonyl oxygen atom O_2^a of the HAc molecule. Two of these bonds (curves a and c) in Figure 11) display a very similar behavior. The third one (curve b) shows an interesting, different behavior. The corresponding time evolution curve of the $O_2^a\cdots H_2$ distance (mean value 2.678 Å) shows two broad maxima in the amplitudes. The large mean value signifies that this hydrogen bond is significantly weaker than the two other hydrogen bonds and the maxima indicate that the whole HAc molecule performs a wagging motion with respect to this bond. A very interesting hydrogen bond is formed between the O_4 and H_1^a atoms (see Figure 4). Figure 12 shows the time evolution of both interatomic distances for this hydrogen bond. The upper, dashed curve represents the time evolution of the $O_4\cdots H_1^a$ distance and the bottom curve gives the time evolution of the corresponding $O_1^a-H_1^a$ bond of the carboxyl group. Several proton-transfer jumps of the carboxyl proton are observed. They are characterized by amplitudes with peaks above 1.3 Å in the bottom curve in Figure 12 and corresponding bottom amplitudes in the upper curve. Vertical thin full lines in this figure indicate

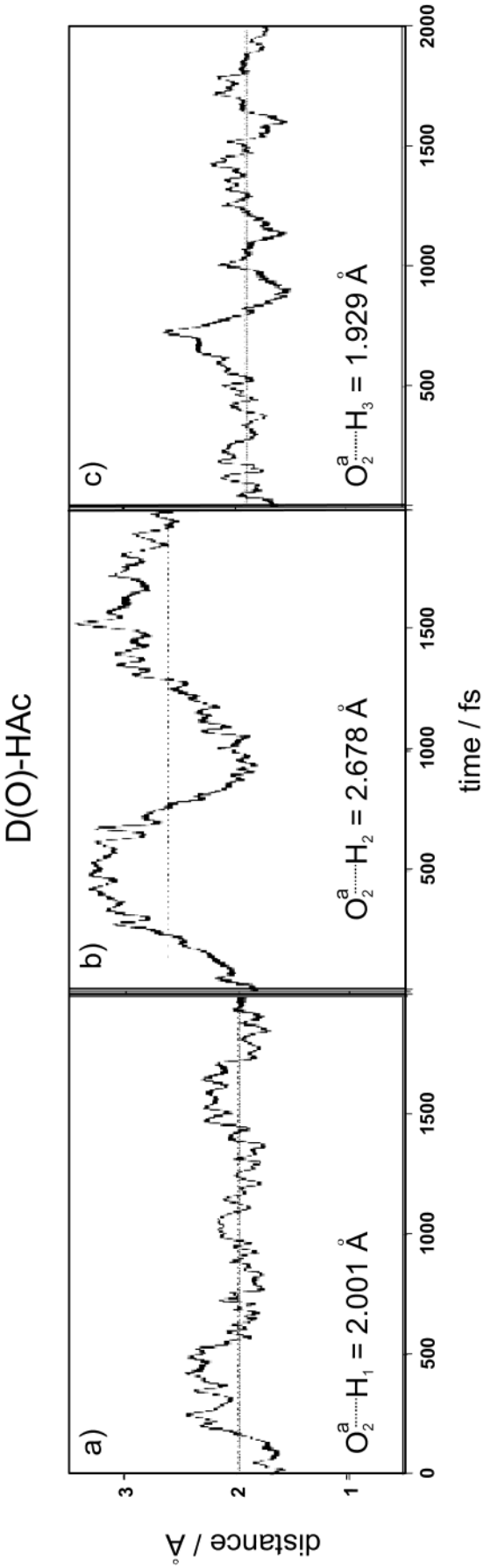

Figure 11. The time evolution of the three hydrogen bonds formed between three surface hydroxyl groups and the carbon: O_2^a of the HAc molecule of the D(O)-HAc system. Horizontal lines indicate mean values and correspond to the numbers given in the figure.

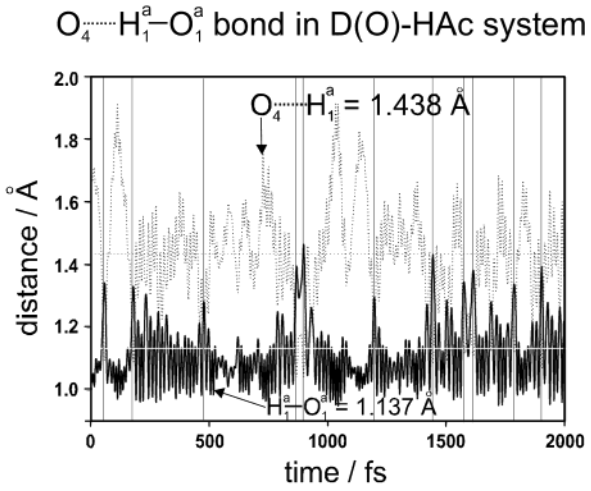

Figure 12. The time evolution of both interatomic distances of the O_4···$H_1{}^a$—$O_1{}^a$ hydrogen bond of the D(O)-HAc system. Horizontal lines indicate mean values and correspond to the numbers given in the figure. Vertical lines indicate proton jumps.

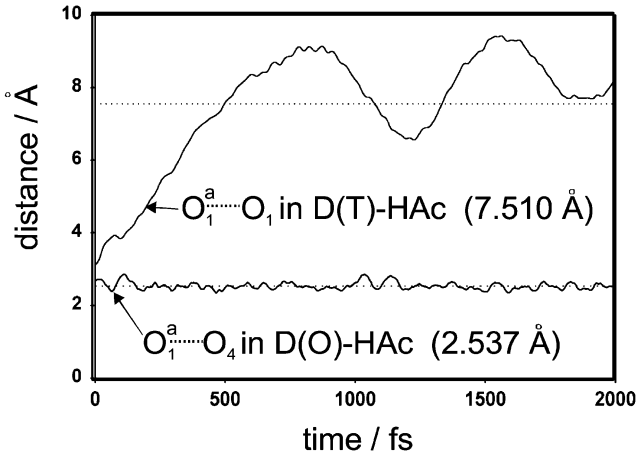

Figure 13. The time evolution of the interatomic distances between the $O_1{}^a$ atom of the HAc molecule and the O_1 atom (labeling according Figure 5) of the D(T)-HAc system (upper curve) and time dependence of the distance between the $O_1{}^a$ atom of the HAc molecule and the O_4 atom of the surface hydroxyl group of the D(O)-HAc system (bottom curve, labeling according Figure 4). Horizontal lines indicate mean values and correspond to the numbers given in the figure.

these incidents. The carboxyl proton jumps to the corresponding surface oxygen atom can be considered as the formation of the short-lived surface hydroxyl groups.

Figure 13 displays the time evolution of the interatomic distances (upper curve in Figure 13) between the $O_1{}^a$ atom of the HAc molecule and the O_1 atom (see the labeling in Figure 5) on the tetrahedral side. The bottom curve is time dependence of the distance between the same atom $O_1{}^a$ of the HAc molecule and the O_4 atom on the octahedral side. The large amplitudes of the upper curve in Figure 13 indicate a very slow translational—rotational movement of the HAc molecule above the tetrahedral hole (similar to the D(T)-H_2O system). On the other hand, the evolution of the $O_1{}^a$···O_4 distance shows strong localization of the HAc molecule at the octahedral surface.

Densities of phonon states for the protons in H_2O and HAc have been calculated and are in the direct line with our observations for the time evolutions of the interatomic distances described above. Figure 14 shows the region of the stretching and bending modes of the water molecule for free H_2O, D(O)-H_2O, and D(T)-H_2O, respectively. The spectrum of free H_2O is primarily given for the purpose of internal reference. In the

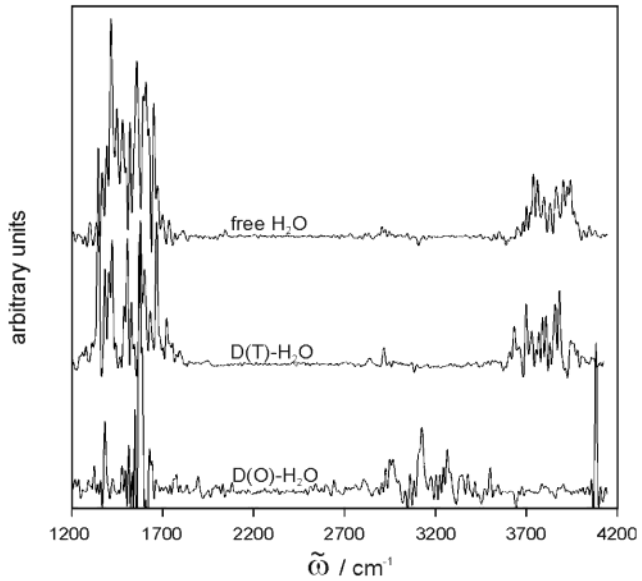

Figure 14. Projected densities of phonon states for the protons of the water molecule for free H_2O, D(O)-H_2O, and D(T)-H_2O, respectively.

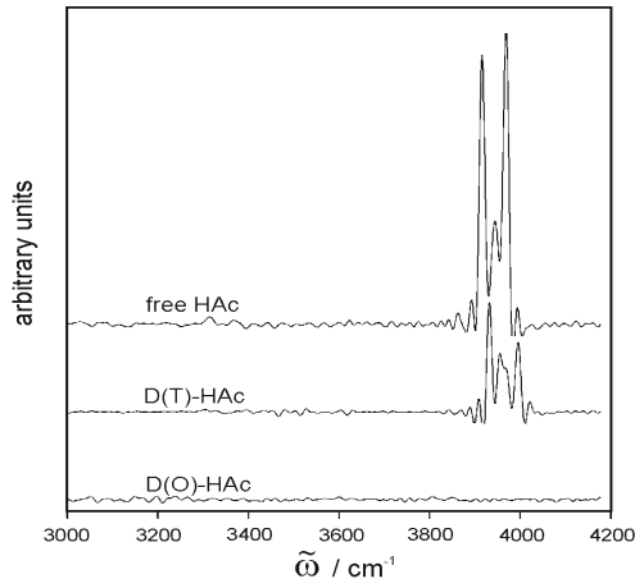

Figure 15. Projected densities of phonon states for the protons of the water molecule for free HAc, D(O)-HAc, and D(T)-HAc, respectively.

experimental spectrum of the water in the gas phase[30] the HOH bending region is found in the interval of 1200−1900 cm^{-1}, in good agreement with our calculated spectrum. The stretching modes are located in the region between 3300 and 3900 cm^{-1}. Thus, for the computed stretching vibrations a shift of about 200 cm^{-1} to higher values as compared to the experimental bands is observed.

The spectrum of the water molecule interacting with the tetrahedral surface is only slightly perturbed in comparison with the spectrum of the free water molecule. On the other hand, the spectrum of water adsorbed on the octahedral surface is changed significantly. A clear splitting of the OH stretching band is observed. One, very sharp band, is shifted to higher frequency around 4100 cm^{-1}. This band corresponds to the vibration of the proton of the water molecule that is not involved in the formation of hydrogen bonds. Several small bands in the interval 2700−3500 cm^{-1} belong to the water proton involved in the hydrogen bond with the oxygen atom of the surface hydroxyl group. These bands reflect the weakening of this OH bond in the water molecule (significantly lower frequencies than in the case of free water molecule) and its strong perturbation by the surface hydroxyl group.

A similar situation as observed for water is found also for the density of states of the proton of the HAc molecule (Figure 15). The shift between the calculated and experimental[30] OH stretching region of the HAc molecule in the gas phase is about 350 cm^{-1} (calculated values are higher). One can again see almost no difference between the spectrum of the free HAc molecule and the HAc molecule in the D(T)-HAc system. On the other hand, in case of the D(O)-HAc this band completely disappeared into the background noise of the spectrum. It correlates with observed proton jumps between carboxylate group and the surface hydroxyl group visualized in Figure 12.

Conclusions

Static relaxation and molecular dynamics simulations at room temperature have been performed for the adsorption of the water and the acetic acid molecules on the octahedral and tetrahedral sides of a kaolinite layer. Calculated structural parameters and interaction energies obtained from static optimizations are in good accord with our previous cluster model studies.[6] Water and acetic acid form several relatively strong hydrogen bonds with the surface hydroxyl groups on the octahedral side with interaction energies of −14.4 and −20.8 kcal/mol, respectively. The molecular dynamics simulation gave a more complex and more detailed picture of the adsorption processes than the static calculations were able to provide. MD confirmed the strong binding of both molecules to the octahedral surface. Strong perturbations of the structures of the adsorbed molecules on the octahedral surface with respect to the structure of the free molecules were found. While the HAc molecule is involved in hydrogen bonds with the surface hydroxyl groups with both the carbonyl and hydroxyl part of the carboxyl group (only the hydrophobic methyl group is noninteracting), the water molecule participates in the hydrogen bonds only with the oxygen atom and one proton. The second water proton is free and is available for the formation of another hydrogen bond, for example, with another water molecule. Therefore, one can expect the formation of several structurally ordered water layers in the contact zone of the liquid water and the octahedral hydroxyl kaolinite surface. On the other hand, molecules on the tetrahedral side of the kaolinite layer are only weakly interacting with this surface. Both molecules perform translational−rotational movement in a shallow potential above the ditrigonal hole. One can expect that the structure of the liquid water interacting with this surface will have a structure very close to the structure of the bulk water.

Generally, we have shown that tetrahedral (001) surface of the kaolinite layer formed from the plane of basal oxygen atoms is of low energy and can be considered as being a hydrophobic surface. Such conclusion was made from the contact angle measurements[31] for the minerals talc and pyrophillite where only such a (001) surface exists. On the other hand, the octahedral surface can be considered as high energy and hydrophilic. Octahedral surface hydroxyl groups have a bifunctional character and can behave in one situation as a proton donor and in another situation as a proton acceptor. MD simulation of the D(O)-HAc system showed relatively strong Brønsted basicity of the surface hydroxyl group on the octahedral (001) surface as exemplified by proton jumps between the HAc molecule and the surface.

Acknowledgment. This work was supported by the Austrian Science Fund, Project P12969-CHE. We are grateful for technical support and computer time at the DEC Alpha server

and the Linux-PC cluster Schroedinger I of the computer center of the University of Vienna.

References and Notes

(1) Kubicki, J. D.; Schroeter, L. M.; Itoh, M. J.; Nguyen, B. N.; Apitz, S. E. *Geochim. Cosmochim. Acta* **1999**, *63*, 2709.
(2) Stumm, W.; Furrer, G.; Kunz, B. *Croat. Chim. Acta* **1983**, *46*, 593.
(3) Fox, T. R.; Comerford, N. B.; McFee, W. W. *Soil Sci. Soc. Am. J.* **1990**, *54*, 1441.
(4) Bhatti, J. S.; Comerford, N. B.; Johnston, C. T. *Soil Sci. Soc. Am. J.* **1998**, *62*, 152.
(5) Rae, J.; Parker, A. In *Enviromental Interactions of Clays*; Rae, J., Parker, A., Eds.; Springer-Verlag: Berlin, 1988.
(6) Tunega, D.; Haberhauer, G.; Gerzabek, M. H.; Lischka, H. *Langmuir* **2002**, *18*, 139.
(7) Sauer, J. *Chem. Rev.* **1989**, *89*, 199.
(8) Lasaga, A. C. *Rev. Geophys.* **1992**, *30*, 269.
(9) Sauer, J.; Ugliengo, P.; Garonne, E.; Saunders, V. R. *Chem. Rev.* **1994**, *94*, 2095.
(10) Car, R.; Parrinello, M. *Phys. Rev. Lett.* **1985**, *55*, 2471.
(11) Blöchl, P. E.; Parrinello, M. *Phys. Rev. B* **1992**, *45*, 9413.
(12) Blöchl, P. E. *Phys. Rev. B* **1994**, *50*, 17953.
(13) Payne, M. C.; Teter, M. P.; Allan, D. C.; Arias, T. A.; Joannopoulos, J. D. *Rev. Modern Phys.* **1992**, *64*, 1045.
(14) Tse, J. S. *Annu. Rev. Phys. Chem*. **2002**, *53*, 249.
(15) Bailey, S. W. Structures of Layered Silicates. In *Crystal Structures of Clay Minerals and Their X-ray Identification*; Brindley, G. W., Brown, G. Eds.; Mineralogical Society: London, 1980.
(16) Zbik, M.; Smart, R. St. C. *Clays Clay Miner.* **1998**, *46*, 153.
(17) Joswig, W.; Drits, V. A. *N. Jb. Miner. Mh.* **1986**, 19.
(18) Kresse, G.; Hafner, J. *Phys. Rev. B* **1993**, *48*, 13115.
(19) Kresse, G.; Furthmülleer, J. *J. Comput. Mater. Sci*. **1996**, *6*, 15.
(20) Jones, R. O.; Gunnarsson, O. *Rev. Mod. Phys.* **1989**, *61*, 689.
(21) Perdew, J. P.; Zunger, A. *Phys. Rev. B* **1981**, *23*, 548.
(22) Perdew, J. P.; Wang, Y. *Phys. Rev. B* **1992**, *45*, 13244.
(23) Kresse, G.; Joubert, D. *Phys. Rev. B* **1999**, *59*, 1758.
(24) Vanderbilt, D. *Phys. Rev. B* **1990**, *41*, 7892.
(25) Kresse, G.; Hafner, J. *J. Phys. Condens. Matter* **1994**, *6*, 8245.
(26) Nosé, S. *J. Chem. Phys.* **1984**, *81*, 511.
(27) Ferrario, M.; Ryckaert, J. P. *Mol. Phys*. **1985**, *54*, 587.
(28) Benco, L.; Tunega, D.; Hafner, J.; Lischka, H. *Am. Mineral*. **2001**, *86*, 1066.
(29) Benco, L.; Tunega, D.; Hafner, J.; Lischka, H. *J. Phys. Chem. A* **2001**, *105*, 10111.
(30) National Institute of Standards and Technology, NIST/EPA Gas-Phase Infrared Database. National Institute of Standards and Technology: Gaithersburg, MD. http://webbook.nist.gov/chemistry.
(31) Schrader, M. E.; Shmuel, Y. *J. Colloid. Interface Sci.* **1990**, *136*, 85.